Eur Spine J (2016) 25:80–95
DOI 10.1007/s00586-015-4089-5

ORIGINAL ARTICLE

Morphological changes in the human cervical intervertebral disc post trauma: response to fracture-type and degeneration grade over time

Ingrid Sitte[1] · Miranda Klosterhuber[1] · Richard Andreas Lindtner[1] · Martin Cornelius Freund[2] · Sabrina Barbara Neururer[3] · Kristian Pfaller[4] · Anton Kathrein[5]

Received: 2 December 2014 / Revised: 20 June 2015 / Accepted: 26 June 2015 / Published online: 19 July 2015

Abstract
Purpose In the first 24 h post-intervertebral disc (IVD) trauma, up to 75 % cell death has been reported. In addition, burst fractures cause post-traumatic disc degeneration by elevated pro-apoptotic and pro-inflammatory gene transcription. Moreover, some patients have pre-trauma degenerative disc disease. The aim of the study was to assess histological changes and cell-death over a time period of up to 1 year caused by mechanical and structural factors.
Methods 116 anterior portions of IVDs of the cervical spine were studied histologically by light microscopy and ultrastructurally by transmission electron microscopy (TEM). The group was investigated with regard to three main parameters: fracture mechanism (compressive vs. tensile/shear loads), degeneration grade (low vs. high) and endplate fracture (with vs. without). Disc architecture (e.g. ruptures) was studied histologically. Cell morphology was examined ultrastructurally to quantify cell-death, healthy and balloon cells. According to ultrastructural observations, two time-groups (up to 6 days vs. later) were established. Statistical analyses were carried out within and between time-groups.
Results Histological changes were obvious in the annulus fibrosus where ruptures with haematoma were replaced by granulation tissue. Significant differences in cell-death were seen in the first few days due to different loads. In contrast to the more degenerated segments, low degenerated ones revealed significantly less cell death with time post-trauma. Interestingly, no difference was found between groups after the sixth day. Cell-death (mean 44 % for all investigated groups) remained high after day 6 post-trauma.
Conclusion IVDs retrieved from low grade degenerated segments revealed a significant recovery, with less cell-death and a partially restored disc matrix, although cell-death remained high. Long-term clinical studies of stabilized segments arising from different fracture mechanisms are required.

✉ Ingrid Sitte
ingrid.sitte@i-med.ac.at

Miranda Klosterhuber
miranda.klosterhuber@i-med.ac.at

Richard Andreas Lindtner
richard.lindtner@i-med.ac.at

Martin Cornelius Freund
martin.freund@i-med.ac.at

Sabrina Barbara Neururer
sabrina.neururer@i-med.ac.at

Kristian Pfaller
kristian.pfaller@i-med.ac.at

Anton Kathrein
anton.kathrein@krankenhaus-zams.at

[1] Department of Traumatology, Medical University of Innsbruck, Anichstr. 35, 6020 Innsbruck, Austria

[2] Department of Radiology, Medical University of Innsbruck, Innsbruck, Austria

[3] Department for Medical Statistics, Informatics and Health Economics, Medical University of Innsbruck, Innsbruck, Austria

[4] Division of Histology and Embryology, Medical University of Innsbruck, Innsbruck, Austria

[5] Department of Traumatology and Sports Medicine, Sankt Vinzenz Krankenhaus Zams, Zams, Austria

Keywords Cell-death · Necrosis · Apoptosis · Chondroptosis · Post-traumatic degeneration · Disc degeneration disease

Introduction

The integrity of the intervertebral disc can be dramatically diminished by traumatic injury or degenerative disc disease (DDD). Disc degeneration is typified histologically by changes at the cellular level [1]. Increased cell proliferation and cell-cluster formation occur, as well as increased cell-death. Gross matrix changes include lamellar disorganization and fissures [1].

Böhler defined a radiological loss of disc height after spinal fracture as a disrupted intervertebral disc [2]. He described conservatively treated spine fracture healing by osteophytes that bridged towards the adjacent vertebrae. Smith and Wamsley reported on subsequent changes which occurred after incision of rabbit discs, with healing of the superficial fibres by proliferating reactions. Closure of the wound by an active fibrous tissue reaction was for the most completed after 4 weeks. These became calcified and before calcification was completed ossification occurred. While the outer annulus fibrosus healed, the inner annulus fibrosus failed to heal [3]. In an ovine model, nucleus pulposus (NP) 5 mm deep incised discs showed significant matrix changes with loss of proteoglycans and collagens 8 months post-operatively and demonstrated a decrease in disc height and marked degeneration of the NP [4]. An incision of 6 × 20 mm caused vessel ingrowths around the annular lesion, cell cloning in the iAF and loss of NP aggrecan and disc height [5]. Moreover, profound post-traumatic disc degeneration was seen when endplate lesions and vertebral fractures were involved. An in vitro rabbit burst fracture trauma model induced programmed cell death by apoptosis in endplate-disc specimens, with caspase-3/7 levels still elevated up to 28 days [6, 7]. Consistent with investigations in mouse tails, apoptosis is dependent on the magnitude and duration of spinal loading [8]. Chondroptosis was introduced by Roach as a variant of apoptotic cell death in chondrocytes [9]. Chondroptosis involves an increase in the endoplasmatic reticulum and the Golgi apparatus, as well as autophagic vacuoles which lead to complete self-destruction of the chondrocyte [9]. Highest numbers of apoptotic and chondroptotic cells were found post compressive fractures, up to 3 days post-trauma, in human IVDs [10]. Moreover, the response of disc cells in patients with different types of trauma (compression versus more tensile and shear loads) resulted in significant differences in disc cell morphologies [10]. Healthy cells were a rarity, with the majority of cells appearing necrotic. A novel disc cell morphology, the balloon cell, could be described post compression trauma. These cells display a homogeneous euchromatin-rich nucleus, enveloped by an osmiophilic nucleus membrane [10]. Cytoplasmic changes varied from mainly intact membrane structures of organelles to severe necrotic changes, with a complete loss of membranes and organelles [10]. In contrast, discs with the pathology of degeneration and herniation presented less apoptosis/chondroptosis [11]. Moreover, in low grade degenerated herniated discs (DG II/III), the balloon cell was routinely found in the iAF and presented itself viable, with the ability to proliferate into clusters [11]. Such nucleus morphologies are seen in many tissues of high activity, e.g., plasma cells of Multiple Myeloma [12]. However, the potential pathogenic role of the balloon cell in different disc pathologies has yet to be established.

The involvement of a pathologically altered IVD, where high degeneration grades (IV/V) are radiologically observed and degenerative disc disease must be expected, leads us to hypothesize different cell responses in fractured segments of lower and higher degeneration grades (DG). Thus, spine fractures were classified into different fracture types (compressive vs. less compressive with more tensile and shear loads) and investigated here with regard to their degeneration grades. The objectives of this study were to assess changes in the different groups with time post-trauma, microscopically and ultrastructurally.

Materials and methods

One hundred and sixteen anterior portions of ninety-five human injured cervical segments were investigated histologically ($n = 113$) and ultrastructurally ($n = 111$). Patients were injured through car accidents, accidents at work or home and during leisure. Fractures investigated in this study are high-energy injuries which are characterized by either compressive load and/or tensile and shear loads, combined with dislocation of bony structures and disc material. A delay in surgery was seen in multiple trauma injuries and due to transport from another hospital to our spine unit. Some fractures were primarily classified as uncomplicated fractures, presenting no dislocation or malposition and no neurological deficits, and treated conservatively. In some fractures due to secondary dislocation, increasing malposition and persisting pain, the treatment plan was changed to a surgical treatment. Mean age of the investigated patient group was 42 years (16–80 years). According to ultrastructural observations this group was split into two time-groups: 0–5 days post-trauma ($n = 59$) and 6 days to 1 year post-trauma ($n = 57$) (Tables 1, 2).

The study and recruitment procedures were approved by the Ethics Committee, Medical University of Innsbruck (Ethics committee: UN 1052; UN 1653; UN 3849). All participants gave written informed consent after a full explanation of study procedures.

Disc samples were removed during routine surgery (anterior approach) following trauma of the cervical spine (C2/3-C7/Th1). Samples were prepared and immediately dissected into three portions from the longitudinal ligament (LL) towards the NP. These were processed for light and transmission electron microscopy.

Imaging Due to pathomorphological criteria, fractures were classified radiologically (X-ray, CT scans) according to Magerl's classification [13]. These are either (A) compression injury, (B1, 2) flexion combined with compression in the anterior disc portion and (B3) extension or (C) rotation injury. The predominating load (more compression or more tensile and shear loads) was evaluated for the anterior disc portion of the investigated segment. Two groups were assessed: fracture group 1 with more compressive loads (A-, B1-, B2- and C-fractures with cranial trauma to the head; $n = 78$) and fracture group 2 with less compression, more tensile and shear loads (B3- and C-fractures; $n = 38$). For all injured segments the degeneration grade was scored radiologically (X-ray, CT scans) [14]. Degeneration grades I-III were defined as low (DG1: $n = 83$) and grades IV–V as high (DG2: $n = 33$). The fracture groups and degeneration groups were investigated within the different time-groups and both time-groups were compared to each other. To address endplate fractures two groups (only low grade degenerated segments were included) were established: EP1 without endplate fracture and EP2 with endplate fracture. Four independent observers (2 traumatologists, 2 radiologists) examined all images; discrepancies in scores were solved by consensus opinion.

Histology Most samples included the anterior LL, the annulus fibrosus (AF) and the NP. These were fixed in 4 % paraformaldehyde, embedded in wax and stained with haematoxylin-eosin [15]. Parts of the samples were fixed in Schaffer solution, embedded in methyl methacrylate (MMC) and stained with Goldner's trichrome [15]. Resin blocks were cut at 4–6 µm thickness, whereas paraffin blocks at 8–10 µm. Sections were evaluated on a Leica DM 6000/DFC 480 using the image software IM500. Morphological features such as disc rupture, vessel ingrowth and cell cluster formations were noted. In addition, cell counts/mm^2 were undertaken by photographing one representative field (oAF, iAF and NP) of view (×10 objective) of haematoxylin-eosin stained sections.

Ultrastructure Disc specimens destined for ultrastructural analysis were taken from the middle part of the anterior portion containing the LL to the NP. These were dissected into 4 cubes (2–3 mm each; A-D). The samples were fixed in 2.5 % glutaraldehyde and post-fixed in 2 % osmium tetroxide. After embedding in Araldite, sections were treated with uranyl acetate and lead citrate [16]. Gold standard Sections (70–100 nm) were examined in a Zeiss EM 10 transmission electron microscope. Both matrix and cell morphologies were assessed. At least 25–60 cells were examined in each sample of the oAF, 20–50 in the iAF and 15–30 cells in the NP. Qualitative and quantitative analysis of disc cell death (apoptosis, chondroptosis and necrosis), balloon and healthy cells (Fig. 9a–f) were recorded using the following criteria:

(a) *Necrotic cell* Loss of integrity of the cell membrane and/or the nuclear membrane, swelling and vacuolization of cell organelles and/or loss of organelle membranes [17, 18].
(b) *Apoptotic cell* Cell shrinking and blebbing of the cell membrane; nuclear condensation (DNA), margination of chromatin and ruffling of the plasma membrane. Apoptotic bodies comprise cell organelles and/or nuclear material enclosed by an intact cell membrane [19–21].
(c) *Chondroptotic cell* Patchy, condensed chromatin; increased endoplasmic reticulum and Golgi apparatus; autophagic vacuoles; blebbing of cytoplasmatic materials/vesicles but no true apoptotic bodies according to the definition of Kerr [9].
(d) *Balloon cell* A rounded homogeneous nucleus (euchromatin) surrounded by an osmiophilic dark nuclear envelope, frequently presenting a nucleolus. Various amounts of rough endoplasmic reticulum (rER), mitochondria and a Golgi apparatus observed [11].

Three independent observers (1 cell biologist, 2 traumatologists) examined all images; discrepancies were solved by consensus opinion.

Statistical analyses

Object characteristics were summarized in percentages as well as presented as median and interquartile range (IQR). Differences between two unpaired groups were assessed using the non-parametric Mann–Whitney *U* test. *P* values <0.05 were considered statistically significant. Threshold analysis was performed using the Mann–Whitney *U* test and visualized by a scatterplot including a trend line using LOESS (LOcal regrESSion) smoothing with an 80 % span. Calculations were performed using SPSS version 20.0 (Armonk, NY, USA) and MedCalc version 15 (MedCalc Software, Ostend, Belgium).

Table 1 Time group 1: Spinal data for 0–5 days post trauma ($n = 59$) including patients details, IVD morphological features and spinal characteristics of IVD segments examined in this study

pat. no / days post trauma	disc age (yrs) / sex	DG of IVD	cervical fracture type	spinal level	disc cell cluster (4 –10 cells)	disc cell cluster (>10 cells)	vessel ingrowths / granul. tissue (GT)	extent of cell death in % oAF iAF NP
1 0	17 m	I	A3.3.	C5/6			oAF	81 58 74
2 0	17 m	I	A3.3.	C6/7			LL	100 92 62
3 0	20 m	I	B1.2.	C3/4				100 93 86
4 0	20 m	I	B1.2.	C4/5			LL,oAF	100 93 92
5 0	25 m	II	A3.3.	C6/7				38 52 75
6 0	25 m	II	A3.3.	C7/ Th1				88 52 89
7 0	33 m	II	B1.2.	C4/5	iAF			73 54 -
8 0	34 m	II	A3.3.	C3/4				- 70 78
9 0	34 m	II	A3.3.	C4/5				44 48 69
10	34 m	II	A3.3.	C5/6	NP		oAF	- 44 31
11 0	39 m	II	C2.1.	C4/5				100 100 100
12 0	41 m	II	C2.1. +	C6/7			oAF	35 43 78
13 0	46 f	II	A3.3.	C4/5				100 72 49
14 0	50 m	III	B1.1.	C4/5				83 83 100
15 0	53 m	II	B1.2.	C6/7	NP			61 43 38
16 0	55 f	III	C2.1.	C6/7	NP			70 55 46
17 0	60 m	II	B3.1.	C4/5	NP		oAF	76 52 86
18 0	62 m	IV	A3.3.	C6/7	iAF NP			87 86 91
19 0	62 m	IV	A3.3.	C7/ Th1				100 87 -
20 0	66 m	III	C2.2.	C6/7	NP			90 89 90
21 0	76 m	IV	B2.3.	C6/7	NP			38 52 64
22 0	77 m	III	B3.1.	C5/6	NP	NP	oAF	13 96 85
23 0	83 m	IV	C2.1. +	C4/5	iAF			- 69 77
24 1	16 m	I	A3.1.	C6/7				66 73 89
25 1	28 m	I	A3.3.	C5/6	NP	NP	oAF	- 47 50
26 1	28 m	I	A3.3.	C6/7				80 83 56
27 1	30 m	I	C2.1.	C4/5			oAF	42 87 77
28 1	31 m	III	C2.1. +	C6/7	iAF		oAF	67 61 58
29 1	33 f	I	C2.1.	C6/7				- 58 84
30 1	45 m	II	C2.1.	C6/7	iAF NP	iAF NP	oAF	87 87 82
31 1	49 m	IV	B2.2.	C6/7	iAF NP			- 54 42
32 1	69 m	IV	B3.1.	C3/4	NP			- 80 46
33 2	16 f	I	C2.1.	C4/5				100 100 -
34 2	26 m	I	C2.1. +	C5/6			oAF	- 62 50
35 2	37 m	I	C2.1.	C6/7				42 78 80
36 2	53 m	II	C2.2.	C6/7				62 70 58
37 2	58 m	II	C2.1.	C6/7			oAF	51 59 47
38 3	25 m	I	B1.2.	C4/5	NP	NP		63 44 64
39 3	25 m	I	B1.2.	C5/6				- 26 57
40 3	30 m	I	A3.3.	C6/7				56 73 46
41 3	30 m	I	A3.3.	C7/ Th1				70 75 88
42 3	31 m	II	B1.2.	C6/7	NP			78 42 75
43 3	35 m	II	B3.2.	C6/7			oAF	63 21 20
44 3	39 m	II	C2.2. +	C5/6				64 70 62
45 3	51 m	IV	B3.1.	C5/6	NP	NP	oAF	60 35 56
46 3	51 m	IV	B3.1.	C6/7	NP	NP	LL,oAF GT in LL	40 37 40
47 4	19 f	I	B1.2.	C6/7			oAF	48 64 46
48 4	35 m	II	C2.1. +	C6/7	iAF		oAF	60 28 -
49 4	43 m	IV	B3.1.	C6/7	NP		oAF	56 39 23
50 4	49 m	III	B3.1.	C3/4	iAF		oAF	52 75 69
51 4	68 m	III	B1.1.	C4/5	NP			74 29 50
52 5	18 m	II	B1.1.	C6/7				48 25 44
53 5	21 f	II	C2.3.	C5/6	NP			65 72 76
54 5	25 m	II	A3.3.	C6/7				92 60 79
55 5	25 m	II	A3.3.	C7/ Th1				90 80 45
56 5	27 m	II	C2.1. +	C4/5			oAF	64 63 69
57 5	54 m	IV	B1.2.	C6/7	NP		oAF	65 55 72
58 5	62 m	IV	C2.2. +	C6/7	iAF NP	NP	oAF,iAF GT in LL	29 34 17
59 5	80 m	IV	B1.1.	C5/6	iAF NP			81 67 -

Cervical fracture classification according to Magerl's system [13]

DG degeneration grade I–V [14], *IVD* intervertebral disc, *LL* anterior longitudinal ligament, *oAF* outer annulus fibrosus, *iAF* inner annulus fibrosus, *NP* nucleus pulposus, *granul. tissue* granulation tissue, "–" not available, "+" compression in the anterior portion of the IVD

Table 2 Time group 2: Spinal data for >6 days post trauma ($n = 57$) including patients details, IVD morphological features and spinal characteristics of IVD segments examined in this study

pat. no / days post trauma	disc age (yrs) / sex	DG of IVD	cervical fracture type	spinal level	disc cell cluster (4 –10 cells)	disc cell cluster (>10 cells)	vessel ingrowths / granul. tissue (GT)	extent of cell death in % oAF iAF NP
1 6	22 f	II	C2.1.	C6/7				48 50 92
2 6	45 f	IV	B3.1.	C5/6			oAF	52 81 69
3 6	55 m	IV	B3.1.	C3/4	iAF		oAF	36 30 61
4 6	58 f	IV	B3.1.	C4/5	iAF			54 45 36
5 6	76 f	IV	C2.1.	C6/7	NP		iAF	48 70 42
6 7	36 m	III	C2.1.	C6/7				39 29 77
7 7	54 m	IV	C2.1.	C6/7	NP		oAF,iAF	52 52 38
8 7	66 m	IV	B1.2.	C4/5	NP		oAF,iAF GT –oAF	67 42 -
9 7	66 m	III	C2.1.	C6/7				43 55 31
10 8	51 f	III	B1.1.	C4/5	iAF NP	iAF NP		26 26 42
11 8	51 f	IV	B1.1.	C5/6	iAF NP			31 25 18
12 9	58 m	III	C2.2.	C2/3	NP		oAF	7 15 29
13 10	40 f	III	B1.1	C2/3			LL	60 49 -
14 10	42 m	III	C2.2. +	C6/7	iAF NP			24 35 25
15 11	36 m	II	C2.1. +	C6/7			oAF	31 33 66
16 11	39 m	III	C2.3. +	C4/5			oAF	56 39 -
17 12	42 m	II	C2.3. +	C6/7	iAF			- 58 63
18 12	70 m	IV	C2.1.	C4/5	NP	NP	oAF	43 28 -
19 12	70 m	V	C2.1.	C5/6	iAF NP		oAF GT-oAF	35 29 33
20 13	18 m	III	B1.2.	C6/7	NP		oAF	13 70 40
21 13	31 m	III	B1.2.	C4/5			oAF	46 38 61
22 13	31 m	III	B1.2.	C5/6			oAF	63 40 -
23 16	29 f	III	B2.2.	C7/ Th1	NP			70 52 46
24 16	47 m	IV	C2.1.	C5/6	iAF NP		oAF GT-oAF	22 9 70
25 17	38 f	II	C2.1.	C6/7	NP			65 90 20
26 18	47 m	IV	C2.1.	C6/7	NP	NP	oAF GT-oAF	26 33 32
27 20	22 m	II	C2.1. +	C5/6	oAF iAF	iAF	oAF	- - -
28 21	38 f	III	B1.1.	C5/6	iAF NP	iAF NP	oAF	38 19 36
29 25	40 m	IV	C2.1. +	C5/6	oAF iAF		oAF	35 33 31
30 27	35 m	III	B3.1.	C3/4	iAF NP		oAF	39 47 46
31 28	30 m	II	B1.2.	C6/7			oAF GT-oAF	61 80 85
32 31	19 m	III	A3.1.	C6/7			oAF GT-oAF	42 38 46
33 31	19 m	III	A3.1.	C7/ Th1			oAF GT-oAF	- - -
34 32	59 m	IV	C2.1. +	C6/7	AF NP	AF NP	oAF GT-oAF	39 40 86
35 35	43 m	III	C2.1. +	C6/7	oAF		oAF	- 32 46
36 35	20 m	II	B1.1.	C7/ Th1				70 95 100
37 36	51 m	III	C2.1. +	C6/7				41 50 46
38 40	76 f	III	B2.2.	C6/7	NP	NP	oAF GT-oAF	- 55 68
39 51	48 m	IV	C2.1.	C6/7	NP	NP	oAF GT-oAF	44 30 22
40 62	27 f	III	B1.2.	C6/7	NP	NP	oAF GT-oAF	66 68 70
41 79	50 m	IV	B1.2.	C5/6	NP		oAF GT-oAF	- - -
42 79	50 m	IV	B1.2.	C6/7	AF NP		oAF GT-oAF	- - -
43 93	36 m	II	B3.1.	C6/7	NP		oAF GT-oAF	42 10 -
44 93	43 f	III	B1.1.	C5/6	NP	NP	oAF GT-oAF	53 31 -
45 93	43 f	III	B1.1.	C6/7	iAF NP	iAF NP	oAF GT-oAF	65 - -
46 105	68 m	V	B1.2.	C3/4			oAF GT-oAF	- 45 31
47 120	47 m	II	B3.1.	C5/6	AF NP	AF		- 33 10
48 124	25 f	II	A3.3.	C6/7	NP	NP	oAF GT-oAF	30 38 65
49 124	25 f	II	A3.3.	C7/ Th1			oAF GT-oAF	- - -
50 166	53 m	III	B3.1.	C4/5	NP		LL,oAF GT-oAF	57 35 25
51 276	57 m	IV	B1.1.	C5/6	iAF NP	NP	oAF GT-oAF	32 53 -
52 276	57 m	V	B1.1.	C6/7	iAF NP	iAF NP	oAF GT-oAF	41 19 -
53 317	46 m	III	C2.1. +	C5/6			oAF GT-oAF	43 27 -
54 317	46 m	III	C2.1. +	C6/7	iAF NP	iAF NP	oAF,iAF GT-oAF	58 27 68
55 365	30 m	II	C2.1. +	C7/ Th1	NP	NP	oAF GT-oAF	51 25 11
56 365	48 m	IV	B3.1.	C4/5	NP	NP	oAF GT-oAF	59 - -
57 365	48 m	V	B3.1.	C5/6	iAF NP	iAF NP	oAF GT-oAF	65 70 38

Cervical fracture classification according to Magerl's system [13]

DG degeneration grade I–V [14], *IVD* intervertebral disc, *LL* anterior longitudinal ligament, *oAF* outer annulus fibrosus, *iAF* inner annulus fibrosus, *NP* nucleus pulposus, *granul. tissue* granulation tissue, "–" not available, "+" compression in the anterior portion of the IVD

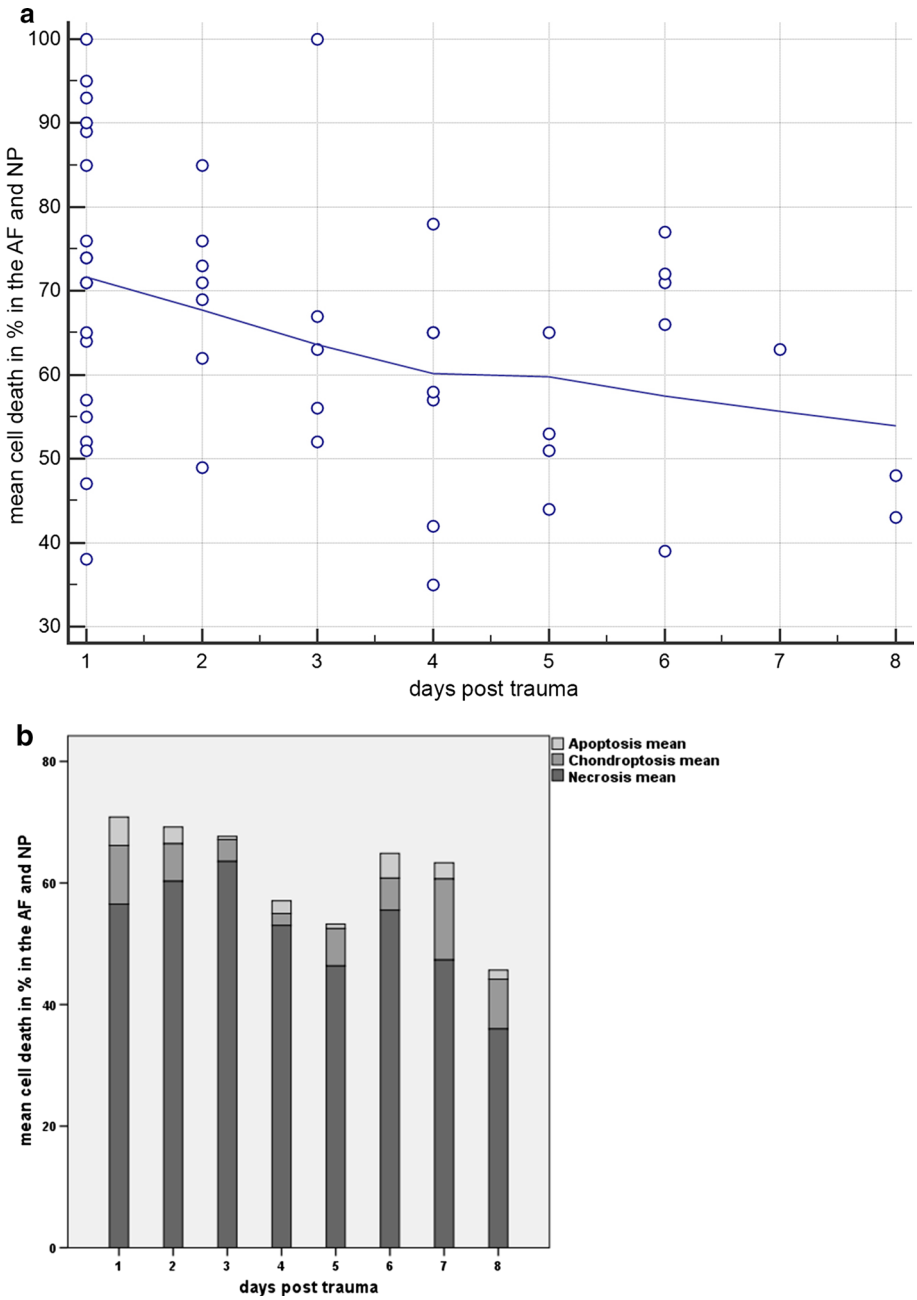

Fig. 1 **a** Scatter plot of cell-death in the first 8 days post-trauma (pt) in percent. Cell-death includes mean values of investigated cell death by necrosis, chondroptosis and apoptosis in the anterior portion of the disc post-trauma. The *line* indicates a trend line using LOcal regrESSion (LOESS) scatter plot smoothing (80 % span). **b** Proportions of cell-death by necrosis, chondroptosis and apoptosis in the first 8 days post-trauma of low grade degenerated intervertebral discs

Results

Ultrastructural investigations revealed considerable differences between day 4 and 6 post-trauma. Whereas micro-ruptures and a disorganized fibril structure were seen in the outer annulus regions in the first days post-trauma, matrix was largely restored with parallel fibrils and less micro-ruptures after the fifth day. Some recovery of disc cells was apparent, with less cell death and more healthy cells and reorganized fibril architecture. Cell proliferation was apparent after day 6. Statistical analyses of the first 8 days of low grade degenerated discs indicated a significant change, to less cell death by necrosis, apoptosis and chondroptosis, after the third day of injury ($P = 0.016$) (Fig. 1a, b). In the two time groups established, (time-group 1 between 0 and 5 days post-trauma and time-group 2 after 6 days post-trauma), no significant difference was found in patients matched for age (Tables 1, 2).

Time-group 1

Imaging Patients with high degeneration grades presented ventral and/or dorsal osteophytes and changes in endplate with signs of severe osteochondrosis. This was not seen in

patients with low grade degenerated discs. A-fractures showed for the most part multiple endplate fractures, which were rarely seen in B- and C-fractures. The alignment of the cervical spine was disturbed (Fig. 2a, c). Twenty-three out of forty-seven low-grade degenerated segments displayed no endplate fracture.

Histology In the first days post-trauma, disc architecture was destroyed, with ruptures with in-bleeding in all compartments of the disc. The normal laminar structure was replaced by radial ruptures in compression fractures. In contrast, C-fractures showed ruptures along the different laminae in the AF (Fig. 3a). Whereas fractures with a low degeneration grade presented a minor number of small cluster formations in the iAF and the NP, more and greater clusters were seen in specimens from patients presenting a higher degeneration grade (Table 1). Some blood vessel ingrowth was apparent in both degeneration groups, coming from the LL and reaching the outer edges of the oAF. Hardly any granulation tissue was seen in discs with high grade degeneration (Fig. 3c). Mean cell count was higher in the AF than in the NP for both fracture groups and degeneration groups (Fig. 4). Significantly higher values of cell counts were present in specimens with high degeneration grades of less compressive fractures, compared to more compressive ones (iAF $P = 0.007$) (Table 3).

Ultrastructure The percentages of different cell morphologies are presented in Fig. 5. Destroyed matrix and damaged cells, including cell debris, were found in the first days post-trauma. Up to 100 % cell-death was apparent in some parts of the injured discs (Table 1). When comparing both *fracture groups*, significantly more apoptosis was seen in the iAF ($P = 0.004$) in compression fractures of low degeneration grade, whereas chondroptosis presented the highest values in the oAF ($P = 0.003$) and NP ($P = 0.038$) (Table 3); significantly less necrosis was seen in the iAF ($P = 0.001$) and NP ($P = 0.016$) than in fractures with more tensile and shear loads. Balloon cells developed a homogeneous nucleus, sometimes a nucleolus and shortly after trauma, some necrotic features in the cell matrix. Significantly more balloon cells were found after compression trauma in the iAF and NP ($P = 0.001$) of discs with minor degeneration than in less compressive fractures.

Comparing the *degeneration groups*, minor differences were seen: for the compression group, the iAF in discs with low degeneration grade presented more apoptosis ($P = 0.028$); less compressive fractures (low degeneration grade) presented significantly more necrosis (NP $P = 0.029$) than discs with a high degeneration grade.

Comparing groups with and without *endplate fracture* and low degeneration grade, significantly more apoptotic cells (iAF $P = 0.019$) and more chondroptotic cells (NP $P = 0.005$) were seen when the endplate was fractured, whereas lesions without endplate fracture showed more necrotic cells (iAF $P = 0.01$; NP $P = 0.02$).

Time-group 2

Imaging Fractures were healed, for the most, 2 months post-trauma with minor signs of endplate sclerosis. Twenty-six out of thirty-five low grade degenerated segments displayed no endplate fractures (Fig. 2b, d).

Histology Vessel ingrowth and granulation tissue were found along the ruptures with time post-trauma in discs with a low degeneration grade, whereas in higher degeneration grades, granulation tissue was all over the AF (Fig. 3b, d; Table 2). More and greater cluster formations were seen in discs of higher degeneration grades. A significant difference in cell count (Fig. 6) was seen comparing the different degeneration grades. An increased number of total cells could be counted in the oAF ($P = 0.013$) when degeneration grade and compression loads were high. Comparing both *fracture groups* with low grade degeneration, no differences were apparent. Significantly more cells were counted post-compression in highly degenerated discs (oAF $P = 0.029$) (Table 3).

Ultrastructure Less cell debris and a largely restored matrix were seen in this time-group. Vessel ingrowths occurred as early as 7 days post trauma with endothelial cells coming from the LL into the oAF (Fig. 9g–i). The percentages of the different cell morphologies are shown in Fig. 7.

No differences comparing both *fracture groups* were seen in low or high grade degenerated discs (Table 3). Interestingly, this time-group presented no differences comparing both *degeneration groups* for compression and less compressive fractures. Low grade degenerated segments with *endplate fractures* did not show differences to lesions without endplate fractures (Fig. 8).

Time-group 1 versus time-group 2

Cell proliferation was found in all compartments due to compression load irrespective of low or high grade degeneration (Table 4). Interestingly, less compressive fractures (low grade degeneration) presented more cell proliferation in the oAF ($P = 0.041$).

Compression fractures in discs with low grade degeneration revealed significantly less apoptosis (iAF $P = 0.005$; NP $P = 0.013$), less chondroptosis (oAF $P = 0.031$) and necrosis (oAF $P = 0.002$; iAF $P = 0.045$) with time post-trauma. In contrast, *less compression fractures* (low grade degeneration) revealed no difference in apoptosis/chondroptosis, and less necrosis in

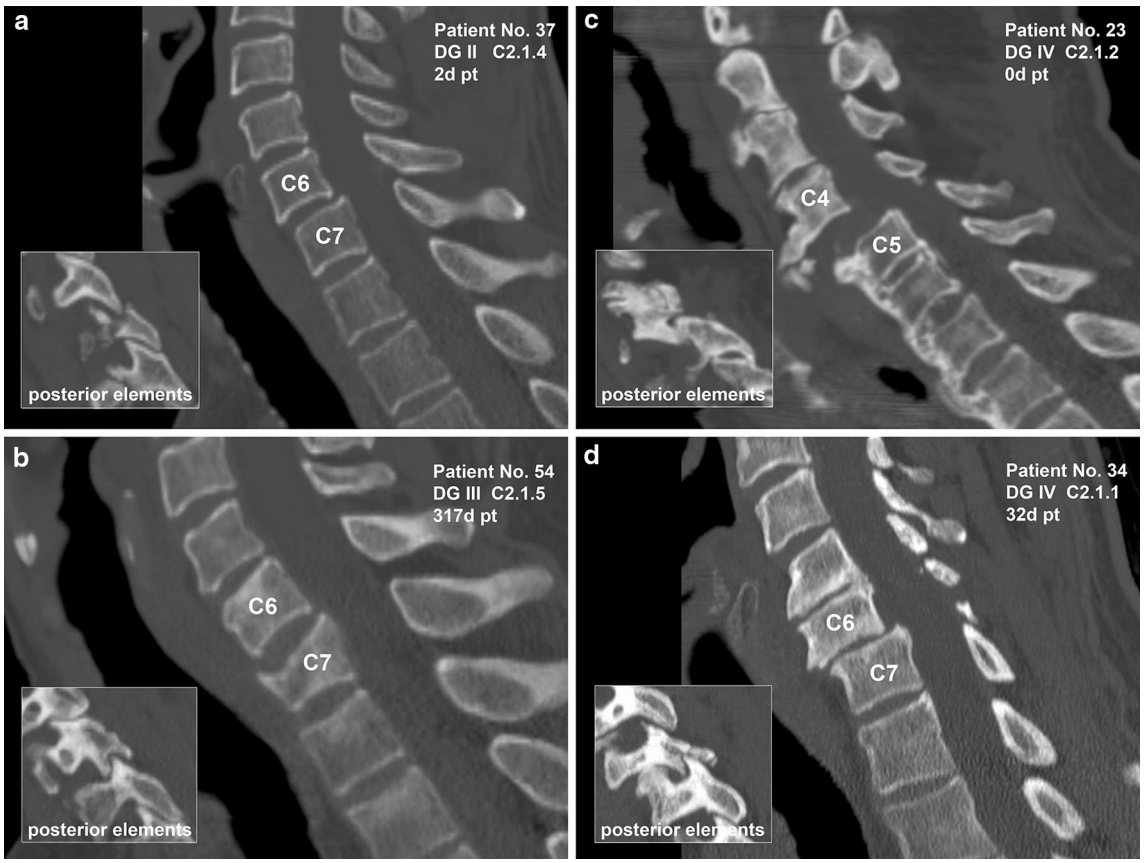

Fig. 2 CT scans illustrating instances of cervical rotation fractures: **a** Patient No 37: rotational anterior dislocation with articular process fracture 2 days post-trauma. *Inset* image presents posterior right fractured articular process. **b** Patient No 54: rotational flexion subluxation with unilateral fracture of the articular process plus type A-fracture 317 days post-trauma with healed anterior compression of the vertebra. *Inset* image presents posterior unilateral healed articular process. **c** Patient No 23: flexion-distraction injury with rotational anterior dislocation 0 days post-trauma. Inset image presents posterior unilateral dislocation. **d** Patient No 34: flexion-distraction injury with rotational anterior dislocation 32 days post-trauma. *Inset* image presents posterior unilateral healed articular process

all compartments (oAF $P = 0.005$; iAF $P = 0.002$; NP $P = 0.005$). Nevertheless, more healthy cells were seen in all compartments in both *fracture groups* and low grade degenerative discs comparing both time groups (Figs. 5, 7).

With higher *degeneration grades* only the iAF displayed less necrosis ($P = 0.043$) and more healthy cells ($P = 0.037$) in compression fractures. No further differences for degeneration grade IV and V discs were found.

Comparing low grade degenerated segments with and without *endplate fracture*, those displaying endplate fractures showed significant differences, having less apoptosis (iAF $P = 0.02$) and less necrosis (oAF $P = 0.002$). In contrast, those without endplate fractures revealed less necrosis in all compartments (oAF $P = 0.003$; iAF $P \leq 0.001$; NP $P = 0.001$). Even though both groups presented more healthy cells (EP1: oAF $P = 0.002$; iAF $P \leq 0.001$; NP $P = 0.001$. EP2: oAF $P = 0.002$) with time post-trauma, some cell-death by apoptosis/chondroptosis and necrosis remained in all investigated groups (Figs. 8, 9d–f).

Overall, cell-death was reduced significantly in most compartments in low grade degenerated discs, but remained high with a median of 43 % (35, 58) for all groups in the oAF [iAF 38 % (29, 52), NP 44 % (31, 68)], similar to high grade degenerated discs.

Discussion

This study reports on 116 post-trauma discs, classified into different groups by injury type and degeneration grade. Acute trauma differed in both fracture groups by either more compression and/or more tensile and shear loads. Intervertebral discs with a low grade degeneration either represent a group of healthy, healthy aged discs, or pathological discs, e.g., an unknown DDD. For IVDs with higher degrees of degeneration, a DDD must be assumed.

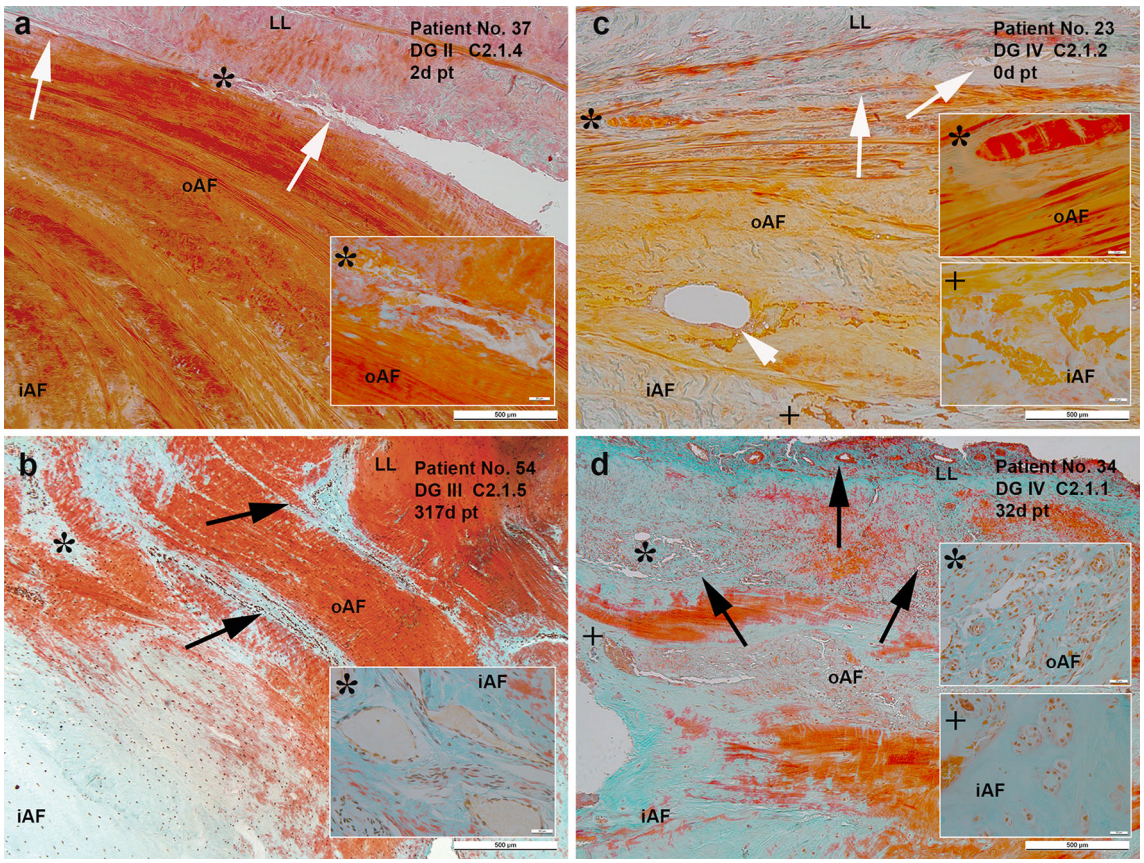

Fig. 3 Histological investigations of less compressive rotation fractures (corresponding to CT scans in Fig. 2). Goldner trichome histology of MMC section presents the outer regions of the intervertebral disc (*scale bar* 500 µm). *Asterisks*/*cross point* out the location of higher magnifications (*scale bars* 20 µm). **a** Patient No. 37 demonstrating outer annular separation (*white arrows*). *Inset* image presents the annular rupture. **b** Patient No. 54 ingrowth of granulation tissue along annular ruptures (*black arrows*). *Inset* image offers vessel ingrowths. **c** Patient No. 23 small outer annular ruptures (*white arrows*) in a disorganized disc. *Inset* image (*asterisk*) presents a rupture containing haematoma; (*small white arrow*) points out an annular degenerative cyst. *Inset* image (*Plus*) shows small ruptures containing haematoma. **d** Patient No. 34 extensive ingrowth of granulation into and around annular ruptures (*black arrows*). *Inset* image (*asterisk*) shows vessel ingrowth surrounded by proliferating cells. *Inset* image (*plus*) presents huge cluster formations. Abbreviations used: *LL* longitudinal ligament, *oAF* outer annulus fibrosus, *iAF* inner annulus fibrosus, *pt* post trauma, *DG* degeneration grade

A limitation of this study might be that instability of an injured segment was not addressed.

High necrosis values were seen in the first days post-trauma and due to compression trauma, high values for apoptosis/chondroptosis with minor differences. The response in the first days post-trauma to compression trauma was almost independent of degeneration grades. For both fracture groups cell-death changed significantly between the investigated time groups, especially in discs with a low degeneration grade. This was not seen in highly degenerated discs. It must be assumed that highly degenerated discs have higher necrosis values prior to trauma [1, 11]. The pathology of degeneration and herniation presented high necrosis values in all compartments of the disc and was similar for all degeneration grades (II–V) [11].

A recent publication revealed lactate dehydrogenase activity, as a marker for necrotic cell death, to be increased up to the third day post-burst fractures in discs of healthy rabbits. Control levels were reached around the fifth day, whereas apoptotic cell death was elevated up to 28 days post-trauma [22]. This was shown for burst fractures, where a structural perturbation of the endplate/IVD was found [22]. Equienergetic loading or nuclear depressurization did not lead to the same results [22]. Our study revealed a significant decrease in cell-death by apoptosis with time post-trauma in the iAF and the NP in low grade degenerated discs, whereas chondroptotic cell death was reduced in the oAF, but remained in some parts of the IVD. Traumatized segments with or without endplate fractures cannot easily be compared between our study and that of Dudli et al. as the mechanism of fractures differed [22]. Nevertheless, fractures without endplate fracture revealed significantly less necrosis and more healthy cells with time post-trauma, but did not differ

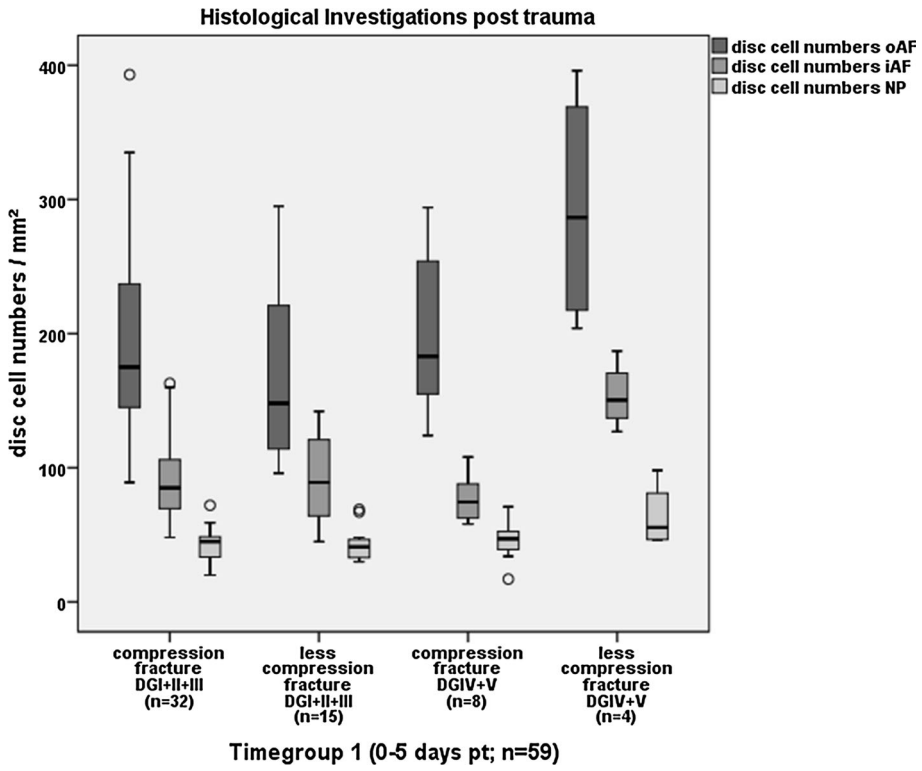

Fig. 4 *Box* and *whisker plots* depicting disc cell numbers/mm^2 identified by light microscopy appearance in the outer and inner annulus fibrosus (oAF, iAF) and nucleus pulposus (NP) of selected IVD specimens, *whiskers* indicate 25 and 75 percentile levels and median values (*horizontal line*) of each sample group. *O* points, which are more then 1.5*IQR from the rest of the data points (outliers)

Table 3 Summary of statistical analysis undertaken in the different time-groups

	Time-group 1 DG I+II+III	Time-group 1 DG IV+V	Time-group 2 DG I+II+III	Time-group 2 DG IV+V
	Compression	Compression	Compression	Compression
	< >	< >	< >	< >
	Less compression	Less compression	Less compression	Less compression
Apoptosis	oAF: P = ns	ns	ns	ns
	iAF: P = 0.004			
	NP: P = ns			
Chondroptosis	oAF: P = 0.003	oAF: P = ns	ns	ns
	iAF: P = ns	iAF: P = 0.029		
	NP: P = 0.038	NP: P = ns		
Necrosis	oAF: P = ns	ns	ns	ns
	iAF: P = 0.001			
	NP: P = 0.016			
Healthy cells	ns	ns	ns	ns
Balloon cells	oAF: P = ns	ns	oAF: P = ns	ns
	iAF: P = 0.001		iAF: P = 0.045	
	NP: P = 0.001		NP: P = ns	
Mean cell count	ns	oAF: P = ns	ns	oAF: P = 0.029
		iAF: P = 0.007		iAF: P = ns
		NP: P = ns		NP: P = ns

ns not significant

compared to those with endplate fracture. This might be caused by prolonged malpositioning with abnormal loads or instability caused by fracture and dislocation of dorsal structures.

Investigations in healthy bovine discs, where discs were traumatized by an impact loading, revealed similar disc cell morphologies and cell-death as found in burst fractures (DGI+II) up to 5 days post-trauma in human cervical

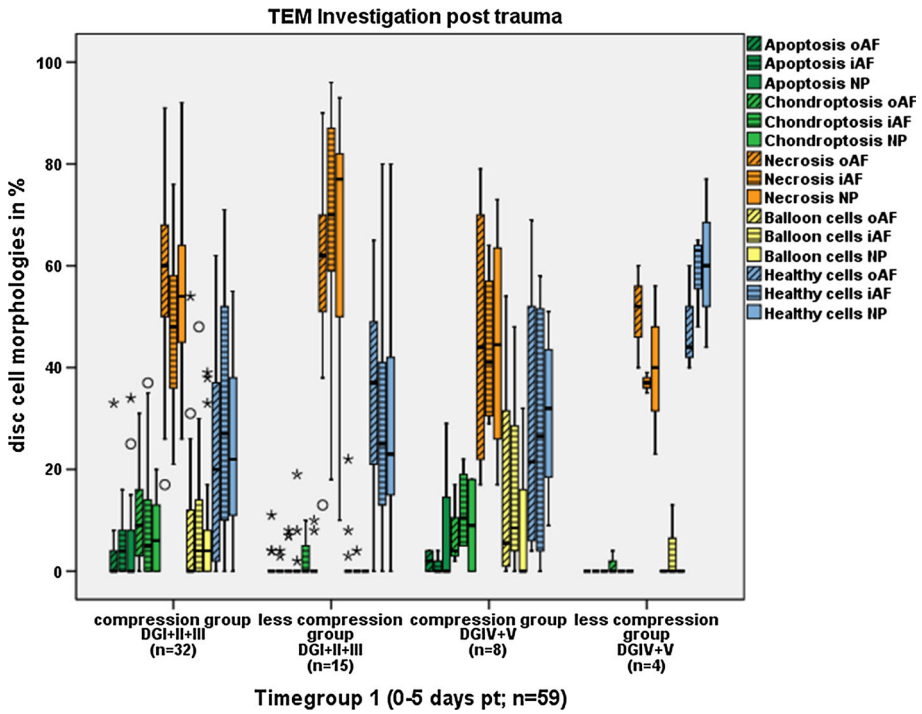

Fig. 5 *Box* and *whisker plots* depicting different cell morphologies identified by ultrastructural appearance—time group 1. The incidence of different disc cell morphologies of the same groups is shown equally for the different disc regions. *Whiskers* indicate 25 and 75 percentile levels and median values (*horizontal line*) of each sample group. *O* points, which are more then 1.5*IQR from the rest of the data points (outliers). *Star* points, which are more then 3*IQR from the rest of the data points (extreme values)

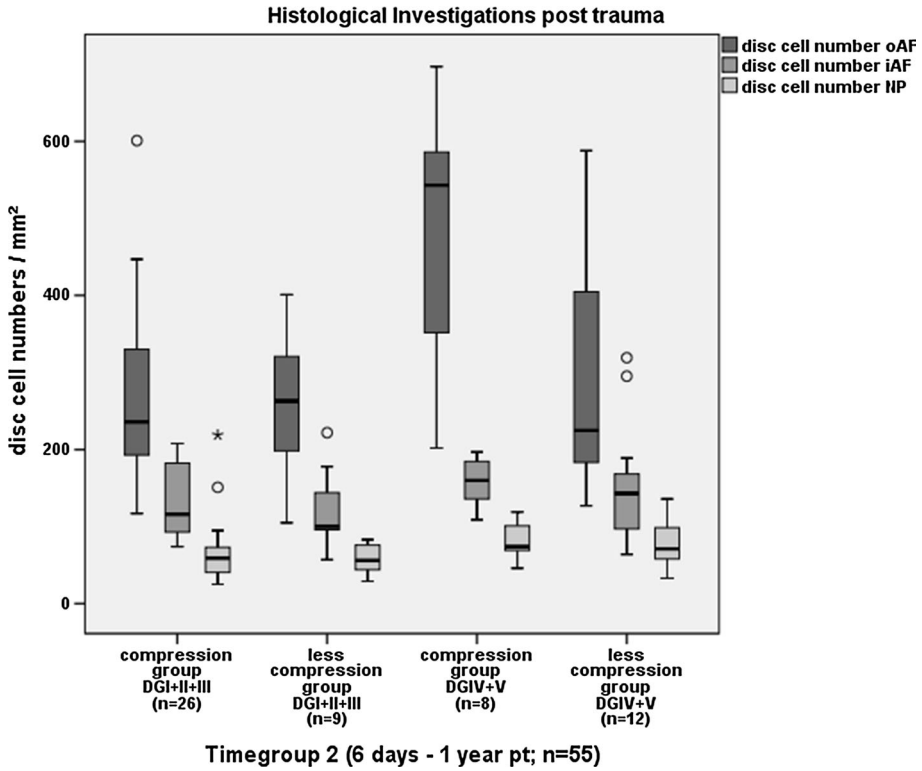

Fig. 6 *Box* and *whisker plots* depicting disc cell numbers/ mm^2 identified by light microscopy appearance in the outer and inner annulus fibrosus (oAF, iAF) and nucleus pulposus (NP) of selected IVD specimens, *whiskers* indicate the 25 and 75 percentile levels and median values (*horizontal line*) of each sample group. *O* points, which are more then 1.5*IQR from the rest of the data points (outliers). *Star* points, which are more then 3*IQR from the rest of the data points (extreme values)

spines [23]. Balloon cells were found within the AF of loaded bovine discs within a distinct range of absorbed energy [23]. It may be hypothesized that increased numbers of balloon cells, especially in the NP of minor degenerated discs, could have additional DDD. At the moment, it is impossible to distinguish balloon cells morphologically as originating from compression or a degenerative disc disease. Battie et al. were able to show with the twin study, that more than 70 % of disc degeneration is based on a genetic influence [24]. Only minor influence was found as a

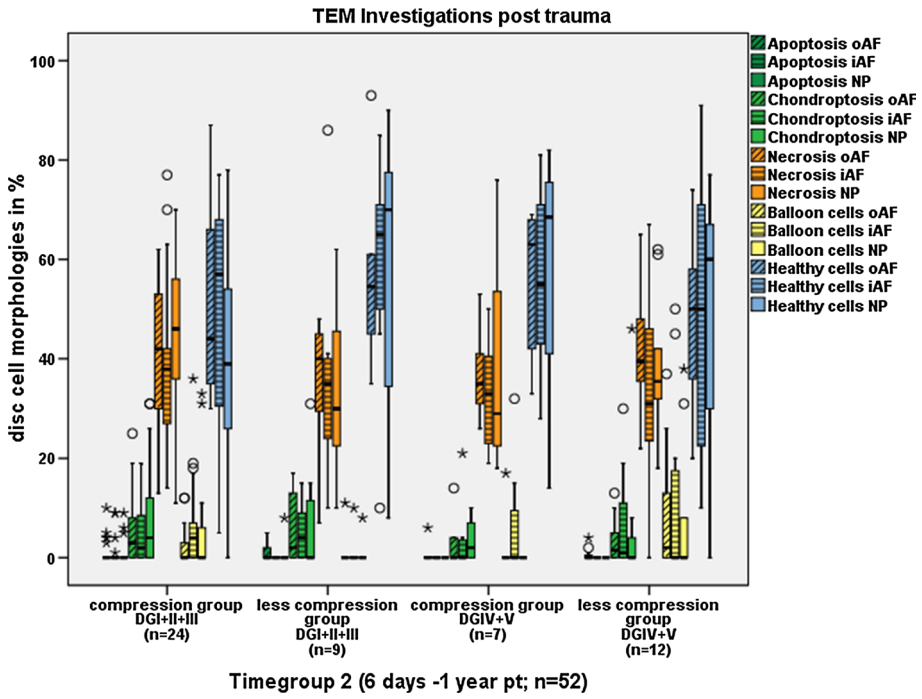

Fig. 7 *Box* and *whisker plots* depicting different cell morphologies identified by ultrastructural appearance—time group 2. The incidence of different disc cell morphologies of the same groups is shown equally for the different disc regions. *Whiskers* indicate 25 and 75 percentile levels and median values (*horizontal line*) of each sample group. *O* points, which are more then 1.5*IQR from the rest of the data points (outliers). *Star* points, which are more then 3*IQR from the rest of the data points (extreme values)

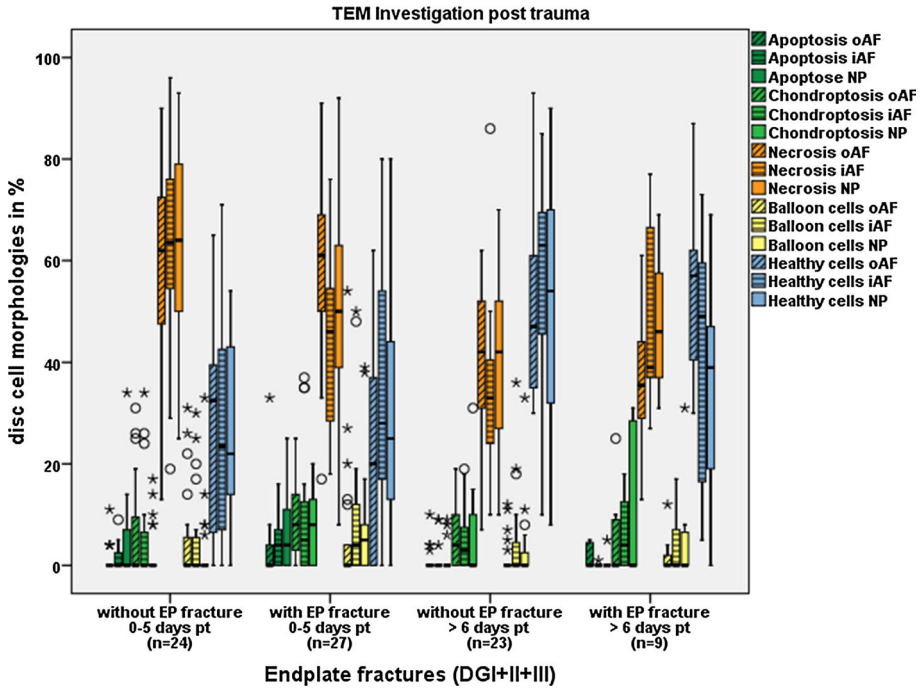

Fig. 8 *Box* and *whisker plots* depicting different cell morphologies identified by ultrastructural appearance in the outer and inner annulus fibrosus and nucleus pulposus of human intervertebral discs with and without endplate fractures in the different time groups. The incidence of different disc cell morphologies of the same groups is shown equally for the different disc regions. The *boxes* show the 25th and 75th percentile and median (*horizontal line*) values. *Bars* show the upper and lower extremes. *O* points, which are more then 1.5*IQR from the rest of the data points (Outliers). *Star* points, which are more then 3*IQR from the rest of the data points (extreme values)

result of ageing and physical loading [24]. Although others report on similar processes such as fragmentation of certain SLRP (small leucine-rich proteoglycans) core proteins (e.g., bigylcans, lumican) in pathological tissues from patients with scoliosis, DDD and herniations, which are important for organization of collagen fibres and hence the structure of the extracellular matrix, the origin of these pathologies is different [25]. Moreover, there is evidence that these are involved in regulating inflammatory pathways [25]. Dudli et al. reported on up-regulation of matrix remodelling genes being stable within 28 days following burst fractures in rabbits [26]. Burst fractures caused a strong up-regulation of pro-inflammatory and a moderate up-regulation of pro-apoptotic genes, with all transcription levels back to control levels after 4 weeks [26]. This group, furthermore, found endplate fracture to be the key

Table 4 Summary of statistical analysis undertaken in the different degeneration groups

	DG I+II+II compression fractures	DG I+II+II less compression fractures	DG I+II+II with EP fractures	DG I+II +II without EP fractures	DG IV+V compression fractures	DG IV+V less compression fractures
	Time-group 1 < > Time-group 2	Time-group 1 < > Time-group 2	Time-group 1 < > Time-group 2	Time-group 1 < > Time-group 2	Time-group 1 < > Time-group 2	Time-group 1 < > Time-group 2
Apoptosis	oAF: P = ns iAF: $P = 0.003$ NP: $P = 0.010$	ns	oAF: P = ns iAF: $P = 0.020$ NP: P = ns	ns	ns	ns
Chondroptosis	oAF: $P = 0.021$ iAF: P = ns NP: P = ns	ns	ns	ns	ns	ns
Necrosis	oAF: $P = 0.001$ iAF: P = ns NP: P = ns	oAF: $P = 0.005$ iAF: $P = 0.002$ NP: $P = 0.005$	oAF: $P = 0.002$ iAF: P = ns NP: P = ns	oAF: $P = 0.003$ iAF: $P \leq 0.001$ NP: $P = 0.001$	oAF: P = ns iAF: $P = 0.043$ NP: P = ns	ns
Healthy cells	oAF: $P \leq 0.001$ iAF: $P = 0.006$ NP: $P = 0.013$	oAF: $P = 0.026$ iAF: $P = 0.004$ NP: P = ns	oAF: $P = 0.002$ iAF: P = ns NP: P = ns	oAF: $P = 0.002$ iAF: $P \leq 0.001$ NP: $P = 0.001$	oAF: P = ns iAF: $P = 0.037$ NP: P = ns	ns
Balloon cells	ns	ns	ns	ns	ns	ns
Mean cell count	oAF: $P = 0.007$ iAF: $P \leq 0.001$ NP: $P = 0.013$	oAF: $P = 0.041$ iAF: P = ns NP: P = ns	oAF: $P = 0.031$ iAF: P = ns NP: P = ns	oAF: $P = 0.012$ iAF: $P = 0.001$ NP: $P = 0.008$	oAF: $P = 0.022$ iAF: $P = 0.001$ NP: $P = 0.018$	ns

ns not significant

aetiological factor for post-traumatic disc degeneration. Nevertheless, compression and/or tensile and shear loads did not disturb the remodelling phase, nor did an insufficient nutrient supply by sclerotic endplates [27]. Moreover, post-trauma studies revealed Caspase 3/7 to be elevated by an increase of the FAS receptor which was only found in post-trauma discs but not in degenerated discs. Up-regulation of the tumour necrosis factor (TNF) receptor was found in both study groups, in post-trauma patients and those with a degenerative disc disease [28, 29]. However, clinical and radiological investigations of traumatic thoracolumbar fractures with endplate fracture, as seen in burst fractures, report on favourable outcomes after stabilization and balloon-assisted endplate reduction up to 6 years post-trauma [30].

Investigations on scoliotic discs of AIS (adolescent idiopathic scoliosis) present an opportunity to study the effects of long-term loading, which is known to result in severely degenerated segments of the affected parts of the spine in elderly patients [31]. The different loading impact has tremendous effects on the IVD and its cells. High numbers of necrotic cells were found on both sides in all compartments, whereas balloon cells were mostly seen on the concave side of these apical discs [32], where more compressive load is expected. Other groups found decreasing rates of cell-death in segments adjacent to apical discs [33]. Dynamic as well as static overload induced early degenerative processes and cell-death in caprine IVDs. Inflammatory related genes were up-regulated [34]. Disruption of the NP and the posterior annulus was histologically obvious in both groups [34]. High mechanical strains promoted secretion of cytokine, inflammatory and neurotrophic factors in human IVD cells, which were associated with DDD [35]. Interestingly, the histology of scoliotic discs presented some vessel ingrowths, some ruptures, but no granulation tissue in this young patient group [32]. Nor did degenerated discs obtained from herniated cervical discs present any granulation tissue in the anterior portion at any degeneration grade, but some vessel ingrowths were surrounded by rare fibrocystic cell invasion [11]. Kokubo et al. described granulation tissue surrounding the hernia in degenerated discs [36]. However, granulation tissue was present in most discs after 3 weeks post-trauma, consistent with incision studies done by others [3, 5, 37]. Disturbance of nutrient pathways by increased sclerosis of the healing endplate may be suggested, and defective healing by granulation tissue resulting in decreased stability of the IVD [37]. As the turnover of disc matrix is very slow [38, 39], a collapse of low grade degenerated discs might appear some years

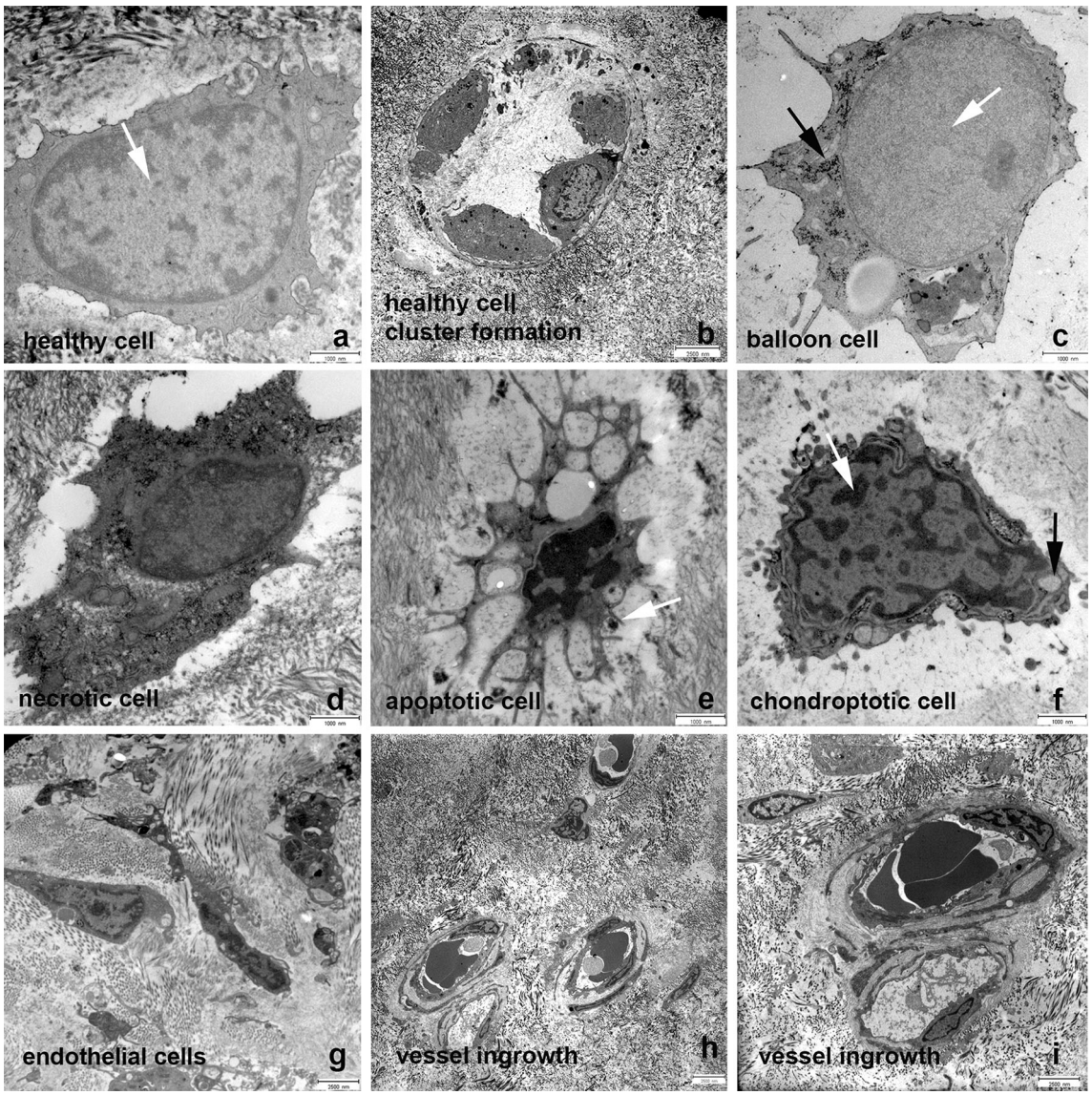

Fig. 9 Different disc cell morphologies in TEM (*scale bar* 1000 nm; 2500 nm in picture **b**, **g**, **h**) of human specimens. Examples of cells with typical morphologies taken in the outer annulus (A): **a** healthy cell: intact cell membrane, good structure of rER and mitochondria. White arrow points towards the heterochromatin of the nucleus. **b** Healthy cell cluster formation. **c** Balloon cell: *Black arrow* points towards storage of glycogen; *white arrow* towards the homogenous nucleus (mostly euchromatin). **d** Necrosis: loss of ER, Golgi apparatus, mitochondria and integrity of membranes. **e** Apoptosis: *arrow points* towards an apoptotic body. **f** Chondroptosis: patchy condensed chromatin (*white arrow*); large vacuoles containing material, which indicates digestion of cellular content (*black arrow*). **g** Endothelial cells migrating into the outer annulus. **h, i** Vessels containing erythrocytes at a higher magnification

post-trauma [40, 41], especially in those with endplate fracture.

Conclusion

This paper is able to show differences in histology with time post-trauma, with granulation tissue ingrowth present in the outer injured regions of the disc and high cell death, mainly by necrosis. As disc lesions are supposed to be similar in the cervical and thoracolumbar spine, the question remains whether reduction and stabilization of a fractured segment is enough to stop high cell-death, found to be similar in both degeneration groups with time post-trauma and independent of the different loads. The survival of an intervertebral disc with a higher degeneration grade and a reduced disc height is doubtful. Long-term clinical follow-up studies of stabilized segments of different fracture types are needed.

Acknowledgments Supported by ÖNB (Österreichische Nationalbank, Jubiläumsfonds—Project Numbers: ÖNB 8590; ÖNB 10032.

Compliance with ethical standards

Conflict of interest The authors do not have any conflicts of interest.

Ethics commission UN 1052; UN 1653; UN 3849. The study and recruitment procedures were approved by the Ethics Committee, Medical University of Innsbruck. All participants gave written informed consent after full explanation of study procedures.

References

1. Roberts S, Evans H, Trivedi J, Menage J (2006) Histology and Pathology of Human Intervertebral Disc. J Bone Jt Surg 88-A:10–14
2. Böhler L (1937) Die Technik der Knochenbehandlung. Band 1. 5. Auflage. Verlag Wilhelm Maudrich Wien
3. Smith JW, Wamsley R (1951) Experimental Incision of the Intervertebral Disc. J Bone Joint Surg 33B:612–625
4. Melrose J, Gosh P, Taylor TKF, Hall A, Osti OL, Vernon-Roberts B, Fraser RD (1992) A longitudinal study of the matrix changes induced in the intervertebral disc by surgical damage to the annulus fibrosus. J Orthop Res 10:665–676
5. Melrose J, Shu C, Young C, Ho R, Smith MM, Gooden B, Dart A, Podadera J, Appleyard RC, Little CB (2012) Mechanical destabilization induced by controlled annular incision of the intervertebral disc dysregulates metalloproteinase expression and induces disc degeneration. Spine 37:18–25
6. Haschtmann D, Stoyanov JV, Gédet P, Ferguson S (2008) Vertebral endplate trauma induces disc cell apoptosis and promotes degeneration in vitro. Eur Spine J 17:289–299
7. Dudli S, Haschtmann D, Ferguson SJ (2012) Fracture of vertebral endplates, but not equienergetic impact load, promotes disc degeneration in vivo. J Orthop Res 30:809–816
8. Lotz JC, Chin JR (2000) Intervertebral disc cell death is dependent on magnitude and duration of spinal loading. Spine 25:1477–1483
9. Roach HI, Aigner T, Kouri JB (2004) Chondroptosis: a variant of apoptotic cell death in chondrocytes? Apoptosis 9:265–277
10. Sitte I, Kathrein A, Pfaller K, Pedross F, Roberts S (2009) Intervertebral disc cell death in the porcine and human injured cervical spine following trauma: a histological and ultrastructural study. Spine 34:131–140
11. Sitte I, Kathrein A, Pedross F, Freund MC, Pfaller K, Archer CW (2012) Morphological changes in disc herniation in the lower cervical spine: an ultrastructural study. Eur Spine J 21:1396–1409
12. Ghadially FN (1997) Ultrastructural pathology of cell and matrix, 4th edn, 4th edn. Butterworth-Heinemann, Boston, Oxford, Johannesburg, Melbourne, New Delhi, Singapore
13. Magerl F, Aebi M, Gertzbein SD, Harms J, Nazarian S (1994) A comprehensive classification of the thoracic and lumbar spine. Eur Spine J 3:184–201
14. Benneker LM, Heini PF, Anderson SE, Alini M, Ito K (2006) Correlation of radiographic and MRI parameters to morphological and biochemical assessment of intervertebral disc degeneration. Eur Spine J 14:27–35
15. Romeis B (1968) Mikroskopische Technik. 16. Auflage. ed. R. Oldenbourg-Verlag, München-Wien
16. David H (1978) Cellular Pathobiology. In: Johannessen JV (ed) Electron Microscopy in Human Medicine, vol 2. McGraw-Hill, New York, pp 114–124
17. Majno G, Joris I (1995) Apoptosis, oncosis, and necrosis. An overview of cell death. Am J Pathol 146:3–15
18. Van Cruchten S, Van den Broeck W (2002) Morphological and biochemical aspects of apoptosis, oncosis and necrosis. Anat Histol Embryol 31:214–223
19. Ihara T, Yamamoto T, Sugamata M, Okumura H, Ueno Y (1998) The process of ultrastructural changes from nuclei to apoptotic body. Vichows Arch 433:443–447
20. Farber E (1994) Programmed cell death: necrosis versus apoptosis. Mod Pathol 7:605–609
21. Kerr JFR, Wyllie AH, Currie AR (1972) Apoptosis: a basic biological phenomenon with wide-ranging implications in the tissue kinetics. Br J Cancer 26:237–239
22. Dudli S, Ferguson SJ, Haschtmann D (2014) Severity and pattern of posttraumatic intervertebral disc degeneration depends on type of injury. Spine J 14:1256–1264
23. Sitte I, Kathrein A, Klosterhuber M, Lindtner RA, Neururer SB, Rauch S, Kuhn V, Schmoelz W (2014) Morphological similarities after compression trauma of bovine and human intervertebral discs. Do disc cells have a chance of surviving? J Orthop Res 32:1198–1207
24. Battie MC, Videman T, Kaprio J, Gibbons LE, Manninen H, Saarela J, Peltonen L (2009) The Twin Spine Study: contributions to a changing view of disc degeneration. Spine J 9:47–59
25. Brown S, Melrose J, Caterson B, Roughly P, Eisenstein SM, Roberts S (2012) A comparative evaluation of the small leucine-rich proteoglycans of pathological human intervertebral discs. Eur Spine J 21:154–159
26. Dudli S, Haschtmann D, Ferguson SJ (2014) Persistent degenerative changes in the intervertebral disc after burst fracture in an in vitro model mimicking physiological post-traumatic conditions. Eur Spine J **(ahead of print)**
27. Grunhagen T, Shurazi-Adl A, Fairbanks CT, Urban JPG (2011) Intervertebral disk nutrition; a review of factors influencing concentrations of nutrients and metabolites. Orthop Clin North Am 42:465–477
28. Heyde C-E, Tschoeke S, Hellmuth M, Hostmann A, Ertel W, Oberholzer A (2006) Trauma induces apoptosis in the human thoracolumbar intervertebral discs. BMC Clin Pathol 6:5–14
29. Tschoeke SK, Hellmuth M, Hostmann A, Robinson Y, Ertel W, Oberholzer A, Heyde CH (2008) Apoptosis of human intervertebral discs after trauma compares to degenerated discs involving both receptor-mediated and mitochondrial-dependent pathways. J Orthop Res 26:999–1006
30. Verlaan JJ, Somers I, Wouter JA, Oner FC (2013) Clinical and radiological results 6 years after treatment of traumatic burst fractures with pedicle screw instrumentation and balloon assisted end plate reduction. Spine J **(ahead of print)**
31. Rajasekaran S, Vidyadhara S, Subbiah M, Kamath V, Karrunanithi R, Shetty AP, Venkateswaran K, Babu M, Meenakshi J (2010) A study of effects of in vivo mechanical forces on human lumbar discs with scoliotic disc as a biological model: results from serial postcontrast diffusion studies, histopathology and biochemical analysis of twenty-one human lumbar scoliotic discs. Spine 35:1930–1943
32. Sitte I, Kathrein A, Pfaller K, Pedross F, Klosterhuber M, Lindtner RA, Zenner J, Ferraris L, Meier O, Koller H (2013) Morphological differences in adolescent idiopathic scoliosis: a histological and ultrastructural investigation. Spine 38:1672–1680
33. Bibby SRS, Fairbank JCT, Urban MR, Urban JPG (2002) Cell viability in scoliotic discs in relation to disc deformity and nutrient levels. Spine 27:2220–2228
34. Paul CPL, Schoorl T, Zuiderbaan HA, Doulabi BZ, van derrVeen AJ, van der Ven PM, Smit TH, van Royen BJ, Helder MN, Mullender MG (2013) Dynamic and static overloading induce

early degenerative processes in caprine lumbar intervertebral discs. PLOS One 8:e62411 **(serial online)**
35. Gawri R, Rosenzweig DH, Krock E, Quellet JA, Stone LS, Quinn TM, Haglund L (2014) High mechanical strain of primary intervertebral disc cells promotes secretion of inflammatory factors with disc degeneration and pain. Arthritis Res Ther 16:R21
36. Kokubo Y, Ushida K, Kobayashi S, Yayama T, Sato R, Nakahma H, Takamura T, Mwaka E, Orwotho N, Bangirana A, Baba H (2008) Herniated and spondylotic intervertebral discs of human cervical spine: histological and immunohistochemical findings in 500 enbloc surgical samples. J Neurosurg Spine 9:285–295
37. Holm S, Baranto A, Holm KA, Ekström L, Swärd L, Hansson T, Hansson HA (2007) Reactive changes in the adolescent porcine spine with disc degeneration due to endplate injury. Vet Comp Orthop Traumatol 20:12–17
38. Sivan S, Tsitron E, Wachtel E, Roughly PJ, Sakkee N, van der Ham F, Degroot J, Roberts S, Maroudas A (2006) Aggrecan turnover in human intervertebral disc as determined by the racemization of aspartic acid. J Biol Chem 28:1309–1314
39. Sivan S, Wachtel E, Tsitron E, Sakkee N, van der Ham F, Degroot J, Roberts S, Maroudas A (2008) Collagen turnover in normal and degenerate human intervertebral discs as determined by the racemization of aspartic acid. J Biol Chem 283:8796–8801
40. Daniaux H, Seykora P, Genelin A, Lang T, Kathrein A (1991) Application of posterior plating and modifications in thoracolumbar spine injuries. Indications, techniques and results. Spine 16:125–133
41. Knop C, Fabian HF, Bastian L, Blauth M (2001) Late results of thoracolumbar fractures after posterior instrumentation and transpedicular bone grafting. Spine 26:88–99